ISSN: 2447-3359

REVISTA DE GEOCIÊNCIAS DO NORDESTE

Northeast Geosciences Journal

v. 11, nº 1 (2025)

https://doi.org/10.21680/2447-3359.2025v11n1ID35730

Refractive Index Analysis in Dam Monitoring: Case Study Hydro eletric power plant Governor Jayme Canet Junior

Análise dos efeitos da refração no monitoramento de barragens Estudo de Caso UHE Governador Jayme Canet Junior

Dayane Wiggers[1]; Pedro Luis Faggion[2]; Wander da Cruz[3]; Andreas Jerke[4]; Samir de Souza Oliveira Alves[5]

[1] Federal University of Paraná/Geomatics Department, Curitiba/PR, Brazil. Email: dayane@ufpr.br
ORCID: https://orcid.org/0000-0001-7339-9436

[2] Federal University of Paraná/Geomatics Department, Curitiba/PR, Brazil. Email: faggion@ufpr.br
ORCID: https://orcid.org/0000-0002-4881-8720

[3] Federal University of Paraná/Geomatics Department, Curitiba/PR, Brazil. Email: wander.cruz@ufpr.br
ORCID: https://orcid.org/0000-0003-0738-1283

[4] Federal University of Paraná/Geomatics Department, Curitiba/PR, Brazil. Email: andreasjerke@ufpr.br
ORCID: https://orcid.org/0000-0002-9476-5201

[5] State University of Rio de Janeiro/Department of Cartographic Engineering, Rio de Janeiro/RJ, Brazil. Email: samir.alves@eng.uerj.br
ORCID: https://orcid.org/0000-0003-3083-0681

Abstract: The influence of atmospheric refraction on dam monitoring is a topic that requires study and discussion, due to variations in atmospheric conditions caused by the region's specific characteristics. The study site is the dam of the Governador Jayme Canet Junior Hydroelectric Plant, located between the municipalities of Ortigueira and Telêmaco Borba, in the state of Paraná. Due to the dam construction, there is a large flooded area, and in the downstream a large roller-compacted concrete (CCR) structure, which absorbs solar radiation throughout the day and results in a significant temperature gradient. The research evaluated the temperature, pressure, and humidity variations throughout the day to calculate monitored point coordinates, which were surveyed using topographic irradiation by total station and automatic target recognition as a search system surveying these. To this purpose, the points surveying was carried out using three different geodetic landmarks, two at the dam upstream and one downstream, to calculate the coordinates of two geodetic landmarks CG01 and CG02 located on the dam crest. The results show that, even after correcting the distances depending on meteorological conditions, the calculated coordinates showed discrepancies and this variation suggests that possible errors may be due to the effects of refraction in the horizontal directions and vertical angles measurements, as we observed a behavior where the average coordinates are more influenced by the point occupied in the survey than by the time of day. Based on the error ellipses analysis, it is possible to verify that the biggest variations were in the morning, which suggests that solar incidence can cause refractive index changes in the region and, therefore, the coordinates.

Keywords: Monitoring of structures; Hydroelectric plant; Refraction.

Resumo: A influência da refração atmosférica no monitoramento de barragens é um tema que requer estudo e discussão, em função das variações das condições atmosféricas causadas por características próprias região. O local de estudo é a barragem da Usina Hidrelétrica Governador Jayme Canet Junior, localizada entre os municípios de Ortigueira e Telêmaco Borba, no estado do Paraná. Em função da construção da barragem a região apresenta uma grande área inundada a montante, o barramento é composto por uma grande estrutura em concreto compactado a rolo (CCR), que absorve a radiação solar ao longo do dia, de forma a gerar um gradiente de temperatura importante. A pesquisa avaliou as variações de temperatura, pressão e umidade ao longo do dia na determinação de coordenadas de pontos de monitoramento, utilizando irradiação topográfica com estação total, juntamente com um sistema de busca automática do ponto a ser monitorado. Para tal, realizou um levantamento, destes pontos, a partir de três marcos geodésicos distintos, dois a montante e um a jusante, com o propósito de calcular as coordenadas de dois marcos geodésicos situados na crista da barragem denominados CG01 e CG02. Os resultados mostram que, mesmo após a correção das distâncias em função das condições meteorológicas, as coordenadas calculadas apresentaram discrepâncias e esta variação sugere que os possíveis erros, podem ocorrer, devido a efeitos da refração nas medidas das direções horizontais e ângulos verticais, pois observamos um comportamento, onde as coordenadas médias são mais influenciadas pelo ponto ocupado no levantamento, do que pelo período do dia. Analisando as elipses de erro é possível verificar que as maiores variações foram no período da manhã, o que sugere que a incidência solar pode causar uma alteração do índice de refração na região e consequentemente nas coordenadas.

Palavras-chave: Monitoramento de estruturas; Usina hidrelétrica; Refração.

Recebido: 25/03/2024; Aceito: 17/05/2024; Publicado: 30/01/2025.

1. Introduction

The periodic monitoring of large engineering structures is essential. In the case of dams, based on Law 12,334/2010 of the National Dam Safety Policy (Política Nacional de Segurança de Barragens - PNSB) (BRASIL, 2010), criteria to guarantee a standard of safety are established, to prevent or reduce the possibility of accidents or disasters and their possible consequences.

To reach the safety standard, it is necessary to carry out inspections, intending to evaluate the structure's physical conditions, seeking to identify and monitor possible failures that may affect it. Then, different methods are available to be applied, depending on the survey precision intended, and the choice of method and equipment used are relevant.

In dam monitoring, it is necessary to consider the lower atmosphere influences (since measurements are carried out at a maximum of 100 meters from the surface), as errors are introduced in this region due to the variation of environmental conditions such as temperature, pressure, and humidity. In hydroelectric power plants (UHE), the dam's purpose is to impound a large quantity of water, to use its potential energy in electrical energy generation. In this way, the region presents specific characteristics, in which the upstream dam has a large area flooded and downstream an area with distinct characteristics, where vegetation is present. In addition, depending on the region of the built dam, it may have an earthen rockfill, a concrete structure, and a spillway (through which water is released when the reservoir reaches its maximum level), among other forms of construction. These characteristics can affect the air mass distribution and the environmental parameters in the survey area consequently.

In the dam region, daily solar radiation can generate irregular thermal gradients, due to heat absorption characteristics, which cause variations in atmospheric conditions in different directions. Depending on the region, this radiation may become encapsulated, generating large temperature, pressure, and humidity variations. Rodriguez (2018 and 2019) distributed sensors on two hydroelectric plants and aimed to verify the temperature behavior in the region. Thereby, it was possible to evaluate different results for each studied region and indicated a possibility of microclimates. During the day, solar radiation can generate temperature gradients due to the absorption of radiation by the structure. Additionally, winds can drive the air mass that remains over the water in the dam's crest and the reservoir area, influencing the temperature of areas near the water surface.

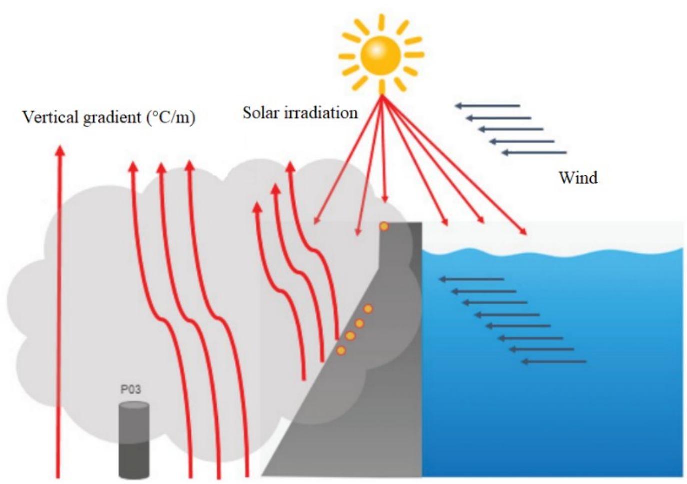

Figure 1 – Temperature gradient scheme in a dam.
Source: Adapted Rodriguez (2018).

Based on the possible varying environmental conditions in the monitored area, it must keep in mind the postulate or principle of “least time”, which means that when an electromagnetic wave travels between two given points, the travel time is minimized. This also means it is the shortest optical path. Remember that the optical path concept is equal to the product of the distance traveled and the local refractive index (HECHT, 1991). In other words, it will be the path with the lowest refractive index. If the refractive index varies perpendicularly to the propagation direction, the ray will be deflected (BOCKEM, et al., 2000).

Atmospheric refraction term describes the change in the electromagnetic wave direction as it propagates through different atmosphere layers near the Earth's crust. When we use a total station, the directions, angles, and distances are obtained by the electromagnetic wave reflection on a target, located at the intended point monitoring. Based on the observation of electromagnetic wave propagations between the instrument and the target, it is essential to know the characteristics of the atmosphere's average density and its gradient during the survey of each (TSOULIS, PETROVIC, KILIAN 2008).

A rigorous density analysis is obtained from the temperature, pressure, humidity conditions, and air composition. The variable access is complex. On the other hand, it is common to measure these parameters punctually and then estimate a density throughout the propagation. Therefore, checking the atmospheric refraction coefficient is fundamental, as well as its observation effects, enabling the determination of the point coordinates surveyed. This helps minimize errors by correcting observations affected by density variations, which generate curvature or deviation of the electromagnetic wave, leading to more accurate observations.

This article presents the studied of these effects in the measurements of the horizontal direction, vertical angle, and inclined distance and, consequently, in the calculation of coordinates over three periods of the day, (morning, afternoon, and night) to evaluate whether due to solar radiation and characteristics topographical information, there would cause in variations in the calculated coordinates.

2. Methodology

2.1 Study Area

The study area is the Governador Jayme Canet Júnior Hydroelectric Plant, previously mentioned as Mauá Hydroelectric Plant. It is located between the municipalities of Ortigueira and Telêmaco Borba, in the state of Paraná state, in Brazil.

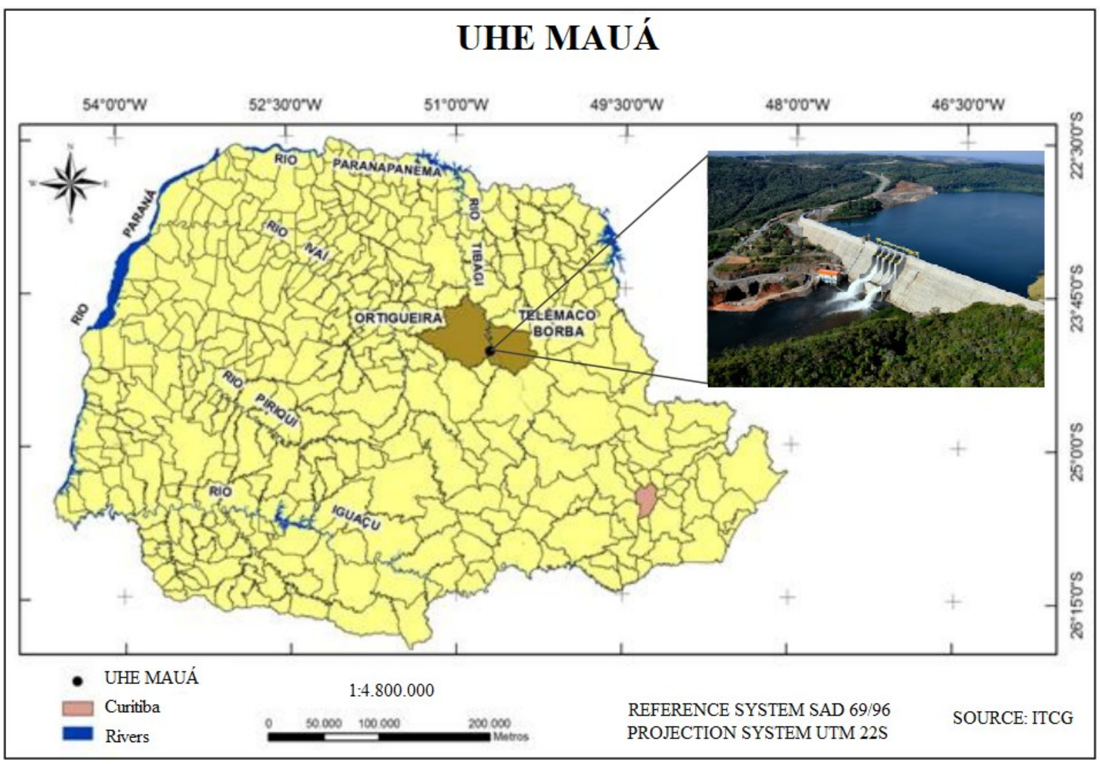

Figure 2 – Localization of study area.
Source: Adapted Siguel (2013).

The dam serves the consumption of approximately 1 million people, located in the Salto Mauá region on the Tibagi River. The concrete dam is 745 m long at the top and 85 m in maximum height, creating a flooded area of 83.9 km² in the reservoir when operated at maximum level, with a normal altitude of 635 m (COPEL, 2021). The study area was chosen as part of a broader project by the Federal University of Paraná in agreement with COPEL (Companhia Paranaense de Energia Elétrica), where it carries out geodetic monitoring of the entire dam.

2.2 Material

The Leica Total Station TS15 was applied to measure horizontal directions, vertical angles, and inclined distances. It can capture data by Automatic Target Recognition (ATR), which enables a prism detection system with greater speed and less operator influence. The equipment has an electromagnetic wavelength of 785 nm to perform the measurement. When operated with the Leica model GPR111, it has an angular measurement accuracy of 1”, and a distance measurement accuracy of ± (1 mm + 1.5 ppm) (LEICA GEOSYSTEMS, 2015).

This equipment is subjected to rigorous verification criteria, with the use of collimators, in addition to a linear base to measure its electronic distance meter. These structures are available at the Geodetic Instrumentation Laboratory (Laboratório de Instrumentação Geodésica - LAIG) at the Federal University of Paraná. The total station could also be classified, ensuring the reliability of the instrument's accuracy.

Temperature, atmospheric pressure, and humidity were measured by a portable meteorological station called Data Logger, whose accuracy in measuring pressure is 0.25%, the temperature is 1 °C, and relative humidity is 5%.

2.3 Data survey

The survey was performed on August 9th and 10th, 2021, in three different positions: two of them upstream and one downstream of the dam. The point called Pillar 01 is located on the right bank upstream of the dam, Pillar 02 is also upstream on the left bank, and Pillar 03 is downstream. The monitored points called CG01 and CG02 are located on the dam crest.

These three pillars were built before finalizing the dam construction to ensure its stability. They were built to its foundation reaches the local rocks. A forced centering system was installed on the top of the pillars, with a standard 5/8” thread compatible with geodetic equipment. This system ensures that equipment or prism may be installed at the same point at different times. According to Nadal (2000), the estimated repeatability in reoccupation using this system is on the order of one-tenth of a millimeter.

Figure 3 – Points used in the surveys (true north).
Source: Adapted from Google Earth (2021).

Figure 4 – Points located on the crest of the dam (CG01).
Source: Authors (2021).

The monitored points are located on the dam crest, which are called CG01 and CG02. The field procedure was based on carrying out six series of readings, in direct and reverse aiming of the telescope (PD, PI). The first series serves to orient to the automatic target recognition system, and the others are performed automatically by the equipment's ATR system. The survey was carried out at three different times: on the 9th in the evening, starting at 7 pm and ending at 11 pm; on the 10th in the morning, starting at 10 am and ending at 1 pm; and in the afternoon, starting at 2:50 pm and ending at 5:20 pm.

Table 1 – Pressure and Humidity Variations.

	Pillar 01		Pillar 02		Pillar 03	
	Pressure (mBar)	**humidity (%)**	**Pressure (mBar)**	**humidity (%)**	**Pressure (mBar)**	**humidity (%)**
Morning	943	47-57	940	34-45	940	30
Afternoon	938	22	939	19	945	23
Night	942	43-52	931	86-90	949	77

Source: Authors (2024).

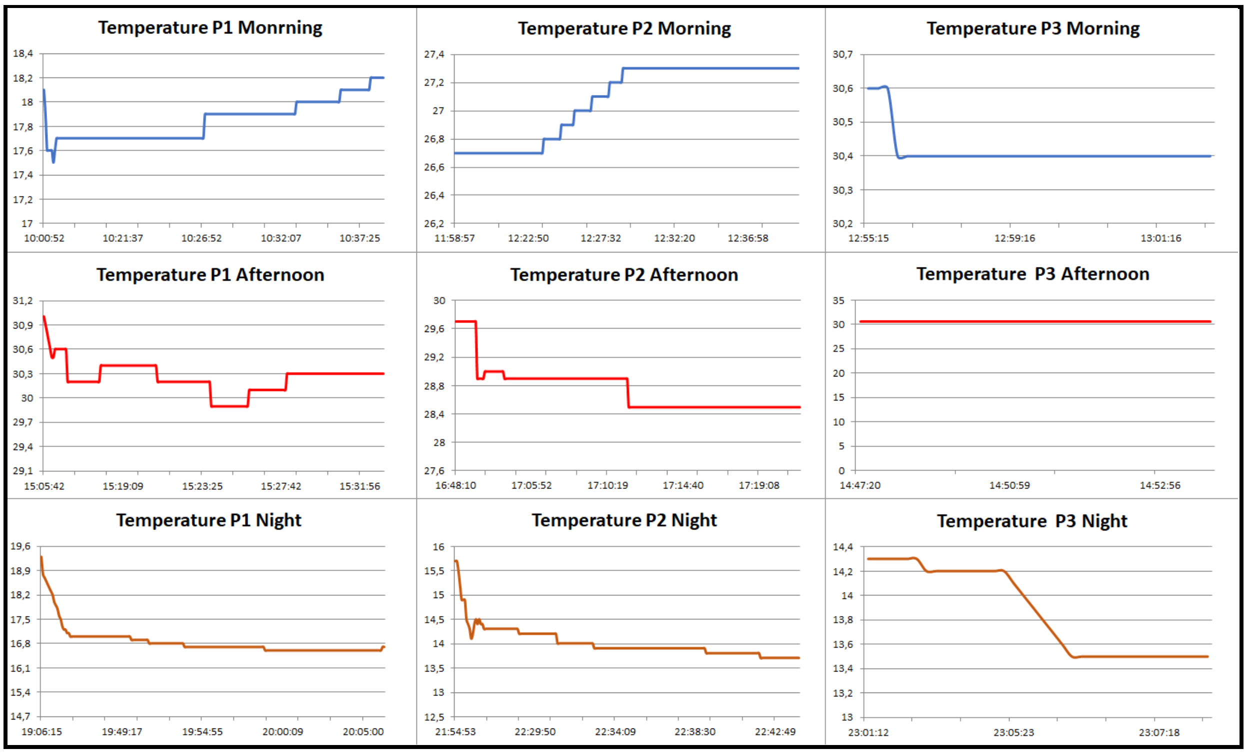

Figure 5 – Temperature variation during the survey.
Source: Authors (2024).

Surveying the points materialized by the prisms (CG01 and CG02) consists of installing the Total TS15 station on Pillar 01, orienting on Pillar 02, and carrying out measurements at the two interest points. Then, the equipment was installed on Pillar 02 and oriented on Pillar 01. Finally, the equipment was installed on Pillar 03 and oriented on Pillar 02. All surveys strictly followed the procedures by the NBR 13.133 (ABNT, 2021).

2.4 Data processing

Subsequently, the data obtained with the total station, according to the instructions indicated in the equipment manual, needed to be corrected for measured distances due to variations in atmospheric conditions (LEICA GEOSYSTEMS, 2015). Knowing this, the data relating to atmospheric conditions were measured by the Data Logger equipment during the surveying of points.

Based on the information about pressure, humidity, and temperature, it was possible to correct the inclined distances, according to equation 1 (LEICA GEOSYSTEMS, 2015):

Equation 1: Atmospheric correction

$$K' = 286{,}34 - \left[\frac{0{,}29525p}{1-\alpha t} - \frac{4{,}126.10^{-4}h}{1+\alpha t}.10^{x}\right]$$

Where: K' = Atmospheric correction in PPM, p = Pressure in mbar or hPa, t = Temperature in °C, h = Air humidity, $\alpha = 1/273{,}15$ e $x = \left(\frac{7{,}5\,t}{237{,}3+t}\right) + 0{,}7857$.

Excel software was applied to correct the inclined distances.

2.5 Reference system used

A Local Cartesian Geodetic System (SGCL) named Barrage System (SB) was established and aimed to facilitate the understanding and coordinate interpretation from the topographic surveys. The "X" axis reference was in the longitudinal direction of the structure with a positive orientation towards the right bank. The "Y" axis was perpendicular to the "X" one and had a positive orientation in the river flow direction (upstream to downstream). The "Z" axis had a positive direction towards the Zenith. More details about the reference system implementation are available on Da Cruz (2015).

Figure 6 – Sketch reference system used (true north).
Source: Adapted Google Earth (2021).

2.6 Calculation of coordinates

Based on the initial coordinates in the SGCL and the vertical angle, horizontal direction, and inclined distance values (corrected according to equation 1) from the 6 series of measured observations, all the coordinates of the surveyed points were calculated by the Position software.

Table 2 – Initial coordinates in the SGCL.

Points	X (m)	σ (m)	Y(m)	σ (m)	Altitude (m)	σ (m)
Pillar 01	903,834	0,001	73,730	0,001	4,629	0,002
Pillar 02	149,123	0,001	142,377	0,001	15,998	0,002
Pillar 03	653,586	0,001	453,844	0,001	-49,976	0,002

Source: Authors (2024).

3. Results and discussion

3.1 Coordinates obtained

According to Dalmolin (2004), all surveying data has errors. In other words, it is impossible to obtain identical values for a set of data, but values are dispersed within a range depending on these errors. As shown in Gemael, Machado, and Wandresen (2015), humans are not the only source of errors; equipment imperfections and environmental conditions that affect the measurements also contribute. In this case, a surveying six observations series had the objective of obtaining a single result, which could represent each point with an appropriate degree of confidence. According to NBR 13.133 (ABNT, 2021), the arithmetic mean of observations is the most likely value when the value is unknown, thus it can be calculated.

As described in Taylor (2012), the useful to estimate the quality of these data is by checking the dispersion of the measurements. Therefore, it is necessary to calculate the standard deviation of the means and evaluate how far these individual values are from the mean value.

The coordinates were calculated for each series of observations and are represented by the mean of the six series for point CG01 and point CG02, with their respective standard deviation values. The data are identified according to the survey period and the position occupied by the total station.

Table 3 – Calculated Coordinates CG01.

CG01	Pillar 01		Pillar 02		Pillar 03	
	X(m)	σ(mm)	X(m)	σ (mm)	X (m)	σ(mm)
Morning	668,6433	0,79	668,6475	1,09	668,6427	3,06
Afternoon	668,6437	0,78	668,6471	0,24	668,6431	1,28
Night	668,6444	0,93	668,6435	0,41	668,6403	0,74
	Y(m)	σ(mm)	Y(m)	σ(mm)	Y(m)	σ(mm)
Morning	207,4342	1,31	207,4382	3,11	207,4313	3,06
Afternoon	207,4359	1,26	207,4352	2,78	207,4324	0,41
Night	207,4339	1,32	207,4346	2,94	207,4328	0,23

Source: Authors (2024).

Table 4 – Calculated Coordinates CG02.

CG02	Pillar 01		Pillar 02		Pillar 03	
	X(m)	σ(mm)	X(m)	σ (mm)	X (m)	σ(mm)
Morning	352,4851	0,80	352,4883	1,39	352,4830	1,97
Afternoon	352,4852	0,66	352,4882	0,52	352,4838	0,82
Night	352,4874	1,86	352,4875	1,22	352,4836	1,29
	Y(m)	σ(mm)	Y(m)	σ(mm)	Y(m)	σ(mm)
Morning	207,0645	1,90	207,0678	1,39	207,0597	2,29
Afternoon	207,0664	2,90	207,0672	0,52	207,0606	1,05
Night	207,0628	2,56	207,0662	1,22	207,0610	1,66

Source: Authors (2024).

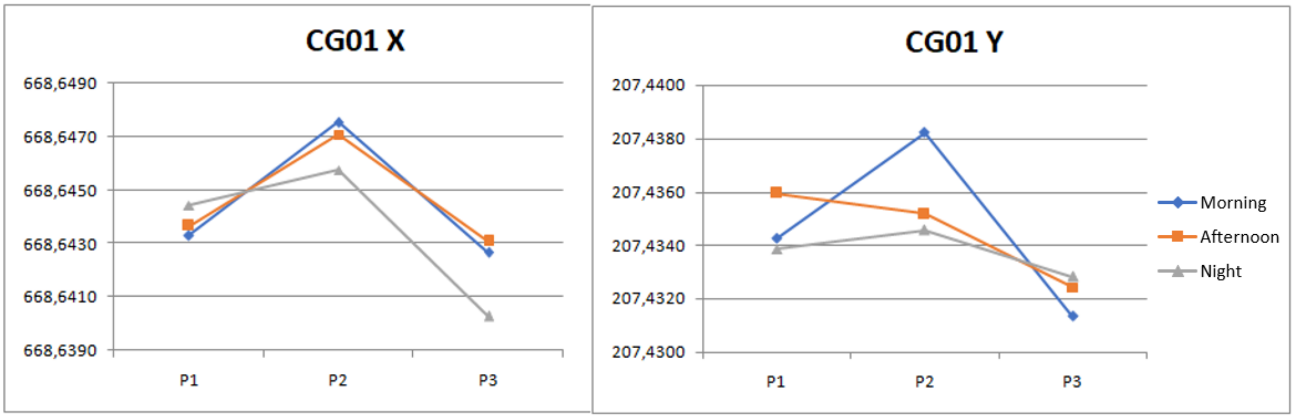

Figure 7 – CG01 coordinates.
Source: Authors (2023).

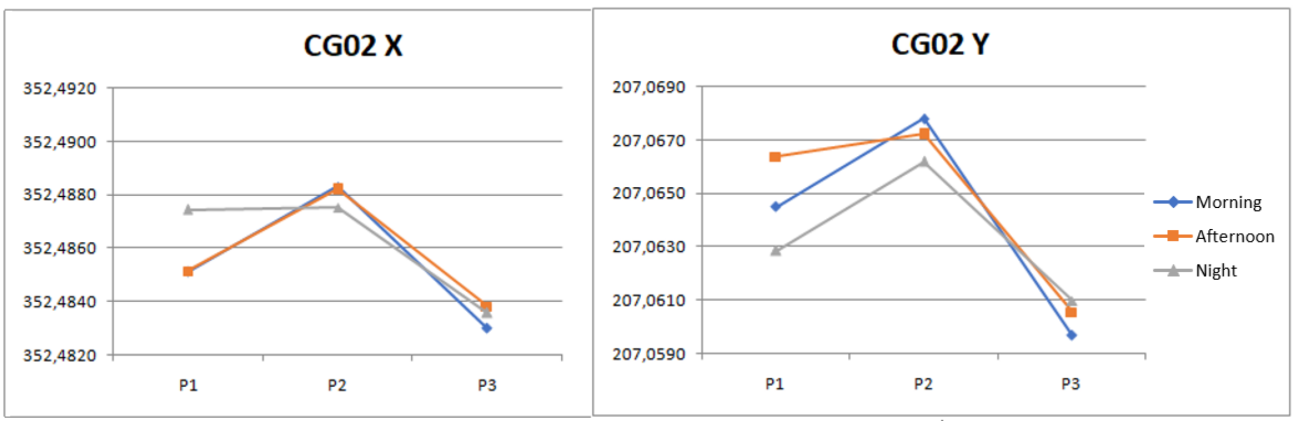

Figure 8 – CG02 coordinates.
Source: Authors (2023).

3.2 Error analysis

Before investigating the accuracy of the calculated coordinates, the accuracy of the distance measurements was analyzed as indicated by NBR 13.133 (ABNT, 2021), which was on the order of 1 mm. After that, errors were propagated to the uncertainty of the coordinates calculated for points CG01 and CG02 on the x and y axes. This was based on the equipment accuracy and the precision of indirect data surveyed (such as instrument and prism height).

Table 5 – Error propagation.

	Pillar 01		**Pillar 02**		**Pillar 03**	
	σ_x(mm)	**σ_y(mm)**	**σ_x(mm)**	**σ_y(mm)**	**σ_x(mm)**	**σ_y(mm)**
CG01	1,4	1,6	1,4	2,6	1,6	1,3
CG02	1,5	2,7	1,3	1,5	1,7	1,9

Source: Authors (2023).

Then, the calculated coordinates were statistically analyzed according to the hypothesis test, considering the surveying time and the occupied point, to verify whether the coordinate means were equal or not. The null hypothesis states that the coordinates are the same. Conversely, the alternative hypothesis indicates the difference between them.

- Null hypothesis H_0: $X_{i,j} = X_{i,j}$
- Alternative hypothesis H_a: $X_{i,j} \neq X_{i,j}$

The coefficients "i" identify the occupied point (Pillar 01, Pillar 02, or Pillar 03), and "j" identifies the period of the surveying (Morning, Afternoon, or Night), so that all combinations are evaluated, excluding those with the same coefficients.

To evaluate the hypotheses, the T Student distribution was used, which according to Gemael, Machado, and Wandresen (2015) is the distribution indicated when the sample has less than 30 elements, it can be calculated from Equation 2.

Equation 2: T Student test:

$$T = \frac{\overline{x_{i,j}} - \overline{x_{i,j}}}{\sqrt{\frac{s^2}{v} + \frac{s^2}{v}}}$$

Where: T = Student's T distribution; $\overline{x_{i,j}}$ = Arithmetic mean of observations (assuming i as occupied location and j period of the day, so that combinations with equal coefficients are excluded); s = Standard deviation of the mean; ; v = degrees of freedom.

In this case, a significance level of 5% was used, assuming the degrees of freedom are equal to 10, we can verify in the T Student's table that the critical value is 2.228. Therefore, all hypothesis combinations were tested considering that the null hypothesis is true for values between -2.228 and 2.228.

According to the critical value, all calculated statistics presented values lower than the established limit. Therefore, the null hypothesis is true for all combinations.

Another statistical analysis performed was the error ellipse. According to Gemael, Machado, and Wandresen (2015), from the variance and covariance matrix, it is possible to estimate the coordinates within a region defined by an ellipse, where the standard deviation of the x and y directions is expressed in numerical values. The mathematical formulation is described in Wolf and Ghilani (1997).

The size of the ellipses is a way of measuring the degree of confidence about the position of the adjusted coordinates. By evaluating the ellipse size, it is possible to determine the uncertainties in x and y.

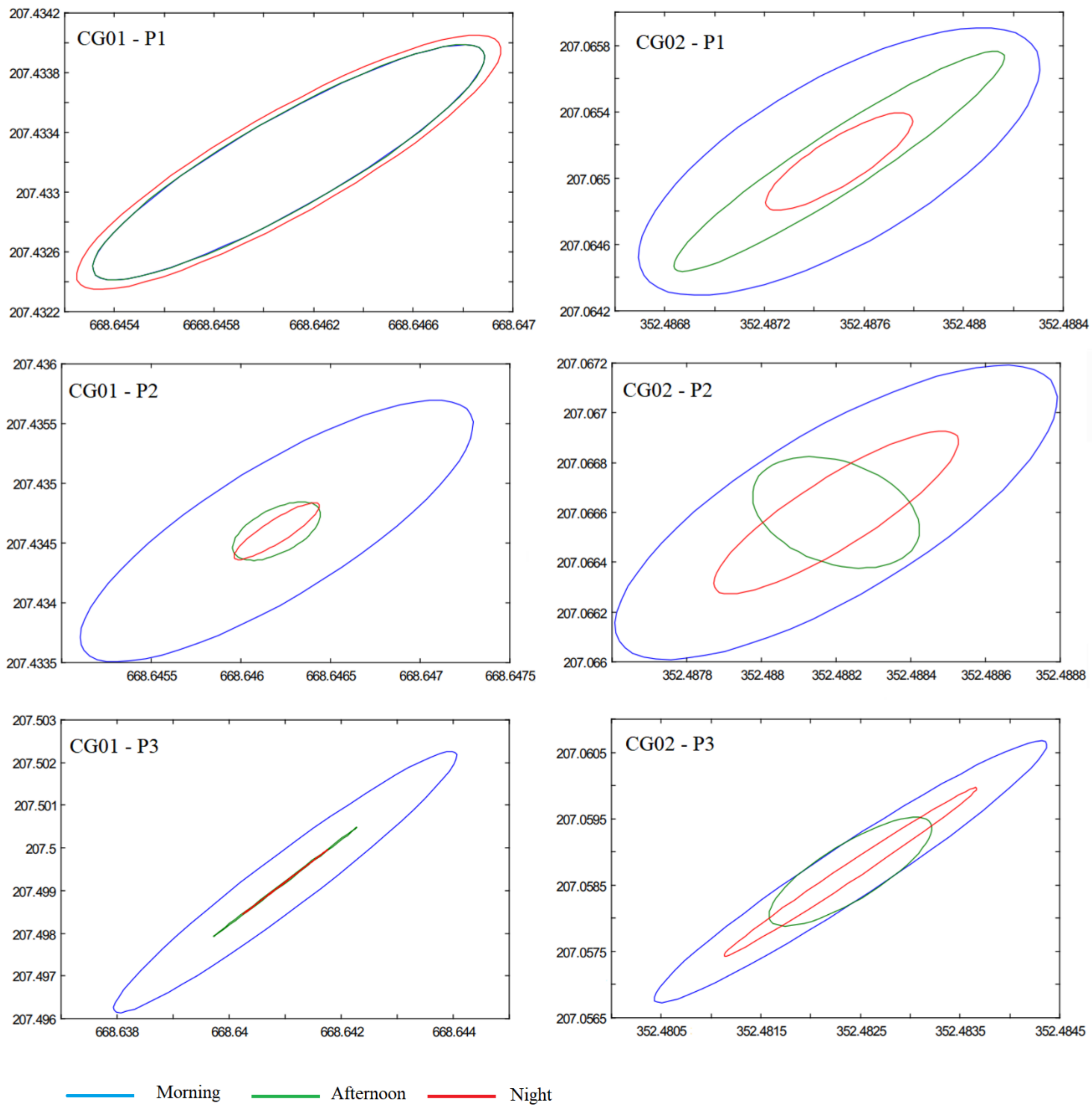

Figure 9 – Error ellipses of points CG01 and CG02 from pillars 01, 02 and 03.
Source: Authors (2024).

4. Final considerations

The CG01 and CG02 coordinates calculated from Pillar 01, Pillar 02, and Pillar 03 were affected by variations during electromagnetic wave propagation. The different atmospheric conditions of each surveying position were the cause. The lines of sight were represented by three different colors: the red line represents the view between Pillar 01 and points CG01 and CG02, the yellow line shows the view between Pillar 02 and points CG01 and CG02, and the blue line represents the view between Pillar 03 and the two CG points.

Because of the height difference of 4 meters between the pillar and the CG points, the line of sight from Pillar 01 is the one that passes closest to the water in the reservoir. In addition to the route being almost entirely above the reservoir.

The line of sight from Pillar 02 has other characteristics. The height difference between the monitored points and the occupied position is approximately 15 meters. This results in the path being far from the water surface. In addition, the line of sight is formed by a mix of vegetation, concrete, and water, with the proportions changing depending on the monitored point. The survey from Pillar 03, which is downstream of the dam, presents a difference in level of approximately 50 meters. Additionally, the line of sight does not follow a path close to the surface, has a smaller water mass, and part of the line is near the dam's concrete surface.

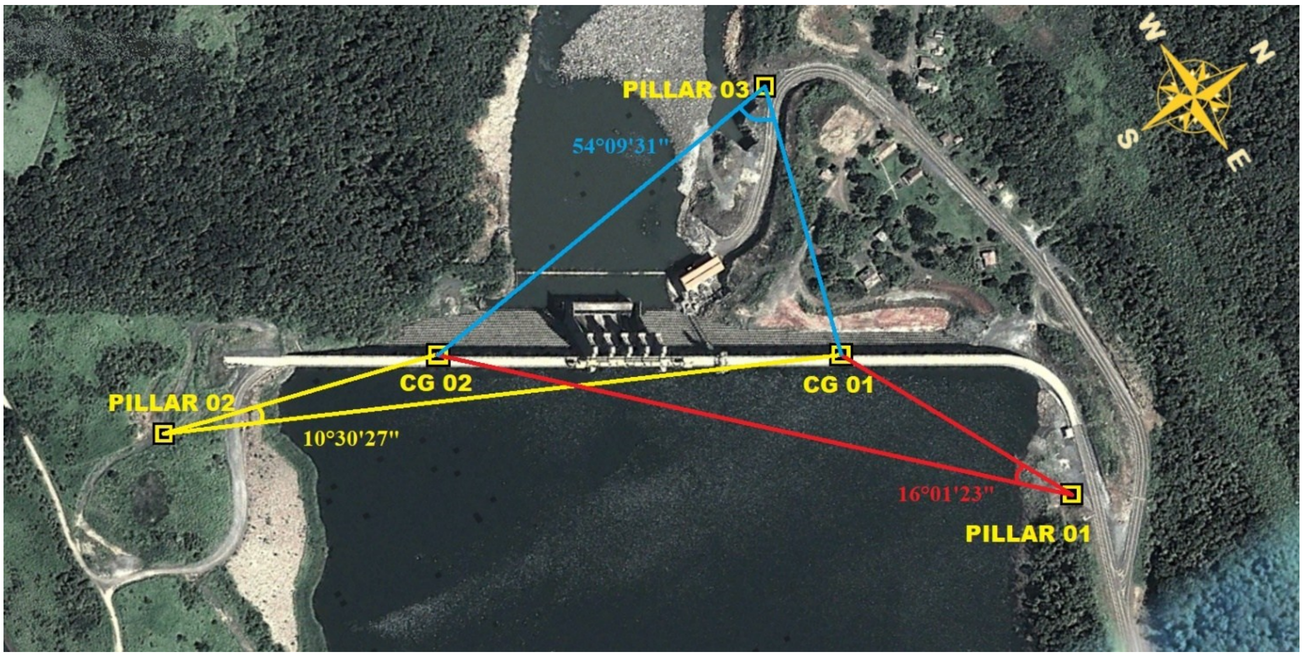

Figure 10 – Lines of sight with their respective angles (true north indication).
Source: Google Earth adapted (2021).

Since the coordinates were obtained after distance corrections, we can establish that their variations come from errors introduced in the measurement process, such as the horizontal and vertical angles. Examining the graphs, the calculated coordinates show that there is no significant variation throughout the day. However, there is a tendency that depends more on the point occupied by the equipment during monitoring. This divergence does not occur when the CG01 coordinates are obtained from P1 in the afternoon and from P2 in the morning, as they present divergent behavior.

All other coordinates show similar behavior, with the lowest coordinate values obtained from Pillar 03 after the coordinate from Pillar 01, and the highest Y coordinate value obtained from Pillar 02.

Verifying this behavior and knowing that the error due to distance variation has already been minimized, it is suggested that possible errors may be due to the effects of refraction in the measurement of horizontal and vertical angles. As previously described, the influence of the distribution of temperature, pressure, and humidity in this region causes variations in the refractive index along the path of the electromagnetic wave. This variation could be a justification for the variations in the calculated coordinates.

Analyzing the error ellipses the biggest variations were in the morning, which is possible to verify in almost all cases (except CG01 from Pillar 01). It suggests that solar incidence can cause a change in the refractive index throughout the surveying period. Following these studies, a more detailed investigation is recommended, with reciprocal and simultaneous observations, to verify the behavior of the coordinates with variations in the refractive index throughout the day.

Acknowledgements

We would like to thank the portgraduate Course in Geodetic Sciences for the opportunity to develop this research, and COPEL for making the area available for study.

Referências

ABNT (Associação Brasileira de Normas Técnicas). NBR 13133: Execução do levantamento topográfico – Procedimento. Rio de Janeiro: ABNT, 2021.

BÖCKEM, B. el al. Refraction Influence Analysis and Investigations on Automated elimination of Refraction Effects on Geodetic Measurements. *XVI IMEKO World Congress*, 2000.

BRASIL. [Lei n°12.334]. *Política nacional de segurança de barragens*. Brasília, DF: Presidente da República, [2010]. Disponível em: https://www.planalto.gov.br/ccivil_03/_ato2007-2010/2010/lei/l12334.htm. Acesso em 02/02/2023

COPEL - Companhia Paranaense de Energia. Geração. 2021. Disponível em: http://www.consorciocruzeirodosul.com.br/a-usina. Acesso em: 20 out. 2021.

DA CRUZ, W. *Integração de dados de monitoramento de estruturas antrópicas. Estudo de caso: UHE Mauá.* Tese (Doutorado em Ciências Geodésicas) Programa de Pós-Graduação em Ciências Geodésicas, Universidade Federal do Paraná, Curitiba-PR, 2015.

Dalmolin, Q. *Ajustamento por Mínimos Quadrados.* 2ª ed. Ed UFPR, 2004. 175p.

Gemael, C.; Machado, A. M. L.; Wandresen, R. *Introdução ao ajustamento de observações: aplicações geodésicas*. 2. ed. Ed. UFPR. 2015. 428p.

Hecht, E. *Óptica*. 1 ed. Lisboa: Fundação Calouste Gulbenkian, 1991. 724p.

LEICA GEOSYSTEMS. Leica TS15. *Manual de operação, versão 3.0, espanhol*. 2015.

NADAL, C. A. *Método da inserção óptica tridimensional aplicado à engenharia de precisao*. Curitiba, 2000. 116f. Tese (doutorado em Ciências Geodésicas). Programa de Pós-Graduação em Ciências Geodésicas, Universidade Federal do Paraná, Curitiba-PR, 2000.

RODRIGUEZ, F. A. C. *Automação da Correção da Primeira Velocidade em Medidas Eletrônicas de Distância com Base um uma Rede de observação de Parâmetros Ambientais Multi-estacões*. Curitiba, 2018. 151f. Dissertação (Mestrado em Ciências Geodésicas). Programa de Pós-Graduação em Ciências Geodésicas, Universidade Federal do Paraná, Curitiba-PR, 2018.

Rodriguez, F. A. C.; Veiga, L. A. K. Desenvolvimento de Interface para Automação da Coleta de Temperatura Baseada em Redes Multiestação Aplicada ao Monitoramento de Estruturas Empregando-se Estações Totais, *Revista Brasileira de Cartografia*. v. 71, n. 3, 781–805, 2019.

SIGUEL, A. R. *Monitoramento da Barragem da Usina Hidrelétrica Mauá Utilizando irradiação Tridimensional*. Curitiba, 2013. 171f. Dissertação (mestrado em ciências geodésicas) - Pós-graduação em ciências geodésicas, Universidade Federal do Paraná, Curitiba, 2013.

Taylor, J.R. *Introdução à Análise de Erros*. Bookman, 2012. 176p.

Tsoulis, D.; Petrović, S.; Kilian, N. Theoretical and Numerical Aspects of the Geodetic Method for Determining the Atmospheric Refraction Coefficient Using Simultaneous and Mutual Zenith Observations. *Journal of Surveying Engineering* V. 134, n. 1, 3-12, 2008.

Wolf, P. R.; Ghilani, C. D. *Adjustment computations: statistics and least squares in surveying and GIS*. 3ed. John Wiley & Sons Inc., 1997. 562p.